

# A Very-Low-Frequency Antenna for Investigating the Ionosphere With Horizontally Polarized Radio Waves<sup>1</sup>

R. S. Macmillan,<sup>2</sup> W. V. T. Rusch, and R. M. Golden<sup>3</sup>

(August 4, 1959)

The advantages of a horizontal half-wave resonant antenna for very-low-frequency propagation experiments lie in its relatively simple and inexpensive construction and in its radiation pattern which is maximum in the vertical direction. The radiation fields of this type of antenna located at the surface of a conducting earth consist of: 1, A horizontally polarized space-wave field radiated in the perpendicular bisector plane of the antenna; and 2, a vertically polarized groundwave field radiated along the axis of the antenna. This vertically polarized field is zero at right angles to the antenna. These fields have been experimentally verified.

The use of a 50-kilocycle horizontal half-wave antenna for vertical-incidence ionospheric sounding experiments is described. The radiation pattern of this antenna is well suited for ionospheric soundings since a receiver located in the groundwave null receives only the reflected skywave signal.

Ground-resistivity measurements made at a number of locations in Central and Southern California were correlated with the geology of the terrain. This correlation showed that the ground resistivity is highest (a condition necessary for optimum antenna efficiency) in areas where the underlying rock formations are relatively unfractured. The amount of annual rainfall and other climatic conditions have little or no effect on the resistivity.

Finally, a unique antenna system is presented which employs resonant loading circuits to convert a section of an existing power line into a horizontal half-wave very-low-frequency transmitting antenna.

## 1. Introduction

A half-wave, horizontal, linear antenna mounted above the ground produces a horizontally polarized radiation field. This type of antenna is relatively inexpensive to construct, requires no tuning elements or ground system, and is well suited for many vlf propagation experiments. It is the purpose of this paper to analyze the radiation properties of this antenna, and to compare these theoretical results with experimental observations. The methods used can be generalized to certain types of more complicated antenna systems. The effects of the underlying geology upon the radiation properties of the antenna have also been considered, and the conclusions reached should be of considerable value in the selection of vlf antenna sites. Finally, a unique system is presented whereby a commercial power line is used as a vlf transmitting antenna.

## 2. Antenna Radiation Fields

The problem of an oscillating dipole located above a plane earth of finite conductivity is of great interest to radio engineers. The classical investigation of this problem was published by Arnold Sommerfeld

[1],<sup>4</sup> who expanded the Hertz vectors from both the primary excitation and the induced secondary effects of the ground in a continuous spectrum of eigenfunctions, and then matched tangential fields at the boundary. In order to match these fields for a dipole parallel to the earth, Sommerfeld has demonstrated the necessity for two components of the Hertz vector,  $\pi_x$  and  $\pi_z$ . Using the coordinates of figure 1:

$$\pi_x = -\frac{e^{ikR_1}}{R_1} + \frac{e^{ikR_2}}{R_2} - \int_0^\infty \frac{2J_0(\lambda\rho)e^{-(h+z)\sqrt{\lambda^2-k^2}}\lambda d\lambda}{\sqrt{\lambda^2-k^2} + \sqrt{\lambda^2-k_E^2}}, \quad (1)$$

$$\pi_z = -\cos\phi \int_0^\infty \frac{2(1-u^2)J'_0(\lambda\rho)e^{-(h+z)\sqrt{\lambda^2-k^2}}\lambda^2 d\lambda}{(\sqrt{\lambda^2-k^2} + \sqrt{\lambda^2-k_E^2})(\sqrt{\lambda^2-k^2} + u^2\sqrt{\lambda^2-k_E^2})} \quad (2)$$

where  $u^2 = k^2/k_E^2$ ,  $k^2 = \omega^2\mu_0\epsilon_v$ ,  $k_E^2 = \omega^2\mu\epsilon + i\omega\mu\sigma$ , and the path of the integration is taken along the real axis of the complex  $\lambda$ -plane. Similar results were obtained by H. Weyl [2] who recognized that the problem could be treated as the reflection and refraction of bundles of plane waves for different angles of incidence at the earth's surface. Unfortunately, (1) and (2) are not readily adapted to numerical computation, and in the years following Sommerfeld's original work, many researchers have attempted to reduce them to more manageable form. A survey of the entire problem is made by J. A. Stratton [3].

<sup>1</sup> This research was supported by the United States Air Force through the Air Force Office of Scientific Research of the Air Research and Development Command under contract No. AF 18(600)-1552, with the exception of the research described in the section on experimental data, which was supported by the Office of Naval Research under contract Nonr.-220(07). The main results of the paper were presented at the Symposium on VLF Radio Waves held in Boulder, Colo., January 1957.

<sup>2</sup> University of Southern California, Los Angeles, California.

<sup>3</sup> California Institute of Technology, Pasadena, California.

<sup>4</sup> Figures in brackets indicate the literature references at the end of this paper

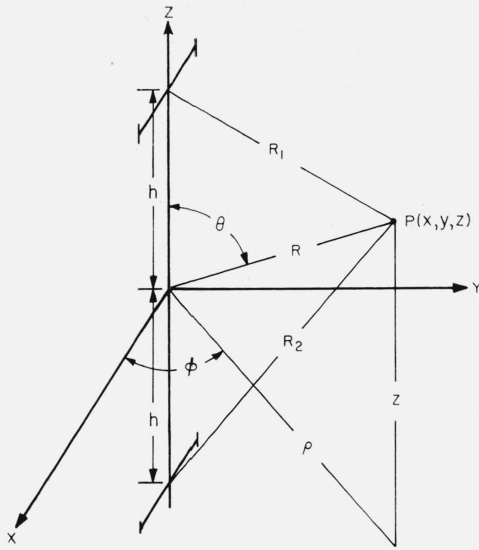


FIGURE 1. Geometry.

K. A. Norton [4] has computed the space and ground waves in the radiation field (i.e.,  $R \gg \lambda$ ) of a horizontal electric dipole located on the surface (i.e.,  $h \approx 0$ ) of a lossy plane earth. From Norton's results, the electric space-wave radiation field in the plane at right angles to the axis of the dipole is:

$$E_x = -ik \left[ \frac{I\eta dx}{4\pi} \right] \left[ \frac{2 \cos \theta}{\sqrt{1/u^2 - \sin^2 \theta} + \cos \theta} \right] \left[ \frac{e^{i(kR - \omega t)}}{R} \right], \quad (3)$$

where  $I$  is the dipole current,  $\eta$  is  $120 \pi$ , the intrinsic impedance of free space, and  $dx$  is the length of the dipole.

In order to compute the corresponding field from a horizontal half-wave antenna, the contributions from each infinitesimal element are integrated along a current distribution  $I_o \cos kx$ . (The justification for assuming this current distribution is presented below.) Then, for the half-wave horizontal antenna located on the surface of a lossy plane earth, the electric radiation field in the plane  $\phi = \pi/2$  is:

$$E_x = \frac{-i\eta I_o}{2\pi} \left[ \frac{2 \cos \theta}{\sqrt{1/u^2 - \sin^2 \theta} + \cos \theta} \right] \left[ \frac{e^{i(kR - \omega t)}}{R} \right]. \quad (4)$$

This horizontally polarized field becomes zero at the surface of the earth.<sup>5</sup> Its radiation pattern (fig. 2) has been verified experimentally (see below) and degenerates into the correct expansion for the equivalent field of a free-space half-wave antenna when  $u = 1$ .

<sup>5</sup> The horizontally polarized groundwave actually varies as  $1/R^2$  but is negligible at vlf [5].

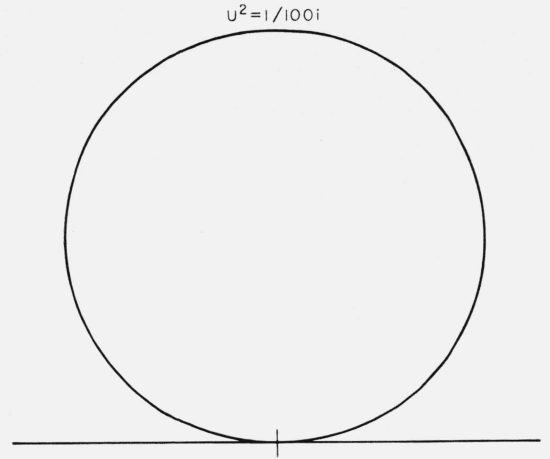


FIGURE 2. Radiation pattern in plane  $\phi = \pi/2$ .

From Norton's results, the electric space-wave radiation field in the vertical plane ( $\phi = 0$ ) of a horizontal electric dipole is:

$$E_\theta = -ik \left[ \frac{I\eta dx}{4\pi} \right] \left[ \frac{2u \cos \theta \sqrt{1 - u^2 \sin^2 \theta}}{\cos \theta + u\sqrt{1 - u^2 \sin^2 \theta}} \right] \left[ \frac{e^{i(kR - \omega t)}}{R} \right]. \quad (5)$$

For a half-wave antenna it is again only necessary to integrate (5) along a half-wave cosinusoidal current distribution to find the field at any angle  $\theta$ . However, in this case the integration must account for the phase differences in the contributions from different sections of the antenna.  $R$  is therefore replaced by  $R - x \sin \theta$  in the exponent. Then, for the horizontal half-wave antenna located on the surface of a lossy earth, the electric radiation field in the plane  $\phi = 0$  is:

$$E_\theta = \frac{-i\eta I_o}{\pi} \left[ \frac{u\sqrt{1 - u^2 \sin^2 \theta}}{\cos \theta + u\sqrt{1 - u^2 \sin^2 \theta}} \right] \times \left[ \frac{\cos \left( \frac{\pi}{2} \sin \theta \right)}{\cos \theta} \right] \left[ \frac{e^{i(kR - \omega t)}}{R} \right]. \quad (6)$$

The radiation pattern of this field in the vertical plane of the antenna is plotted in figure 3. Equations (6) and (4) are identical when  $\theta = 0$ .

At the surface of the earth the field of a horizontal electric dipole consists entirely of the groundwave since the space wave becomes zero when  $\theta = \pi/2$ . Conversely, the groundwave rapidly becomes negligible with increasing height. The dominant component of the groundwave of the horizontal electric dipole is vertically polarized:

$$E_z = ik \left[ \frac{I\eta dx}{4\pi} \right] \left[ \cos \phi u \sqrt{1 - u^2} 2F \right] \left[ \frac{e^{i(kR - \omega t)}}{R} \right] \quad (7)$$

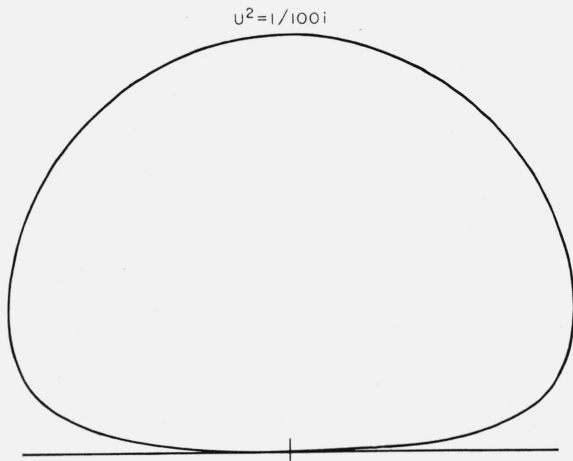


FIGURE 3. Radiation pattern in plane  $\phi=0$ .

where

$$F=1+i\sqrt{\pi w} e^{-w} \operatorname{erf}(-i\sqrt{w}) \quad (8)$$

and

$$w=\frac{ikRu^2(1-u^2)}{2} \quad (|w| \text{ is the numerical distance}). \quad (9)$$

There is a radial component of the groundwave field, smaller than the vertically polarized component by a factor of  $u\sqrt{1-u^2}$  (the "wave-tilt"). There is also a  $\phi$ -component, smaller than the vertical component by a factor of  $u^3$  at large distances, which can be neglected for practical values of earth conductivity.

Integration of (7) along the antenna yields the vertically polarized groundwave field in the plane  $\theta=\pi/2$ . In evaluating the integral,  $R$  is replaced by  $R-x \cos \phi$  in the exponent. The groundwave field of a horizontal half-wave antenna located at the surface of a lossy plane earth is then:

$$E_z = \frac{i\eta I_0}{\pi} \left[ u\sqrt{1-u^2} \right] \left[ \frac{\cos \phi \cos\left(\frac{\pi}{2} \cos \phi\right)}{\sin^2 \phi} \right] \times \left[ F \right] \left[ \frac{e^{i(kR-\omega t)}}{R} \right]. \quad (10)$$

This vertically polarized groundwave field in the horizontal plane of the antenna is maximum along the axis of the antenna and zero at right angles to the antenna. The radiation pattern of this vertical field is plotted in figure 4. Horizontal components of the groundwave field can be neglected for small values of the wave-tilt. Equation (10) was also derived by Wait [5].

Examination of (7) yields information on the properties of the groundwave. For large values of

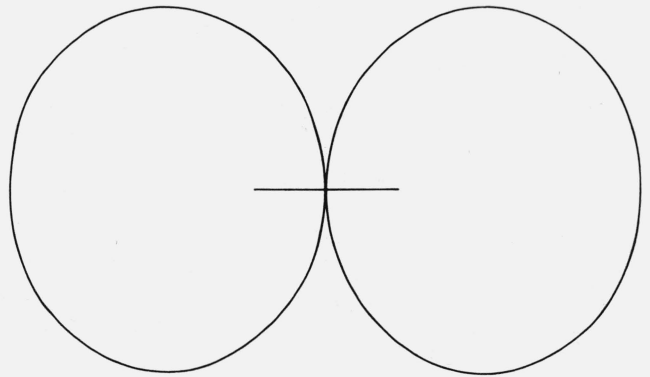


FIGURE 4. Surface-wave radiation pattern in plane  $Z=0$ .

$R$ ,  $F$  asymptotically approaches  $-\frac{1}{2} w$ , and hence the groundwave ultimately varies inversely as the square of the distance. In the vicinity of the antenna, the value of  $F$  is unity, and the groundwave varies inversely as the first power of the distance. A complete discussion of the radial attenuation properties of the groundwave is presented in [4] and [6].

The fields in a plane perpendicular to the center of the antenna ( $\phi=\pi/2$  plane) can also be obtained by considering the superposition of the directly radiated fields and the fields reflected from the plane of the earth.

From the expression for a half-wave antenna in free space, it is seen that the entire electric field is perpendicular to the plane  $\phi=\pi/2$ . Hence it is possible to apply the laws of reflection and refraction to this field. This method can be applied to many more complicated field problems, which would otherwise be difficult to solve.

The geometrical configuration for the path of the direct and reflected fields at distances great compared to the height of the antenna is shown in figure 5(a). By properly matching the fields at the surface of the earth, and neglecting the attenuation due to the small difference in the path lengths, one obtains an expression for the total electric field of the form

$$E_{\text{total}} = (1 + \rho e^{-i\delta}) E_{\text{direct}}, \quad (11)$$

where

$E_{\text{direct}}$  is the free space field in the plane  $\phi=\pi/2$  of a half-wave antenna and equals

$$\frac{\omega\mu_0 I_0}{2\pi k R}$$

$$\rho = \frac{u \cos \theta - \sqrt{1-u^2 \sin^2 \theta}}{u \cos \theta + \sqrt{1-u^2 \sin^2 \theta}}, \text{ reflection coefficient.}$$

$$\delta = \frac{4\pi h}{\lambda_0} \cos \theta, \text{ phase delay of reflected wave.}$$

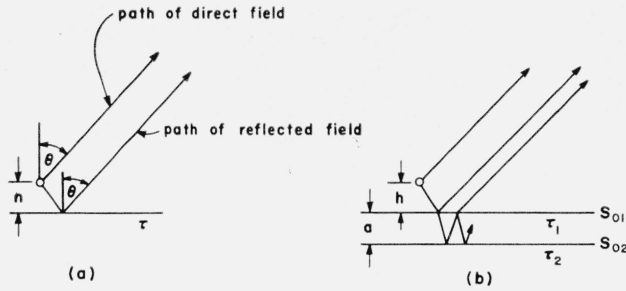


FIGURE 5. Geometrical configuration for the reflection method.

For cases in which the height of the antenna is small compared to a free space wavelength, the ratio of the total electric field in the plane  $\phi = \pi/2$  to the corresponding field in free space is given approximately by:

$$\frac{E_{\text{total}}}{E_{\text{direct}}} = 1 + \rho = \frac{2 \cos \theta}{\cos \theta + \sqrt{1/u^2 - \sin^2 \theta}} \quad (12)$$

Equation (12) is the same as the previously derived eq (4).

This derivation has assumed a perfectly homogeneous earth. In many locations, however, rock of high resistivity is covered by a mantle of low resistivity soil. Hence this case will now be considered.

A homogeneous earth is assumed to be covered with a layer of thickness "a" which has a much lower resistivity than the material that it covers, as shown in figure 5(b).

The reflection method is still useful for this case since the infinite series obtained due to multiple reflections and refractions at the two surfaces  $S_{01}$  and  $S_{12}$  can be readily summed. One thus obtains for the ratio of the total field to the direct field:

$$\frac{E_{\text{total}}}{E_{\text{direct}}} = 1 + e^{-i\delta} \left[ \frac{\rho_{01} + \rho_{12} e^{-i\delta_a}}{1 + \rho_{01}\rho_{12} e^{-i\delta_a}} \right] \quad (13)$$

where

$$\rho_{01} = \frac{u_1 \cos \theta - \sqrt{1 - u_1^2 \sin^2 \theta}}{u_1 \cos \theta + \sqrt{1 - u_1^2 \sin^2 \theta}}$$

reflection coefficient for waves reflected from  $S_{01}$ .

$$\rho_{12} = \frac{u_2 \sqrt{1 - u_1^2 \sin^2 \theta} - u_1 \sqrt{1 - u_2^2 \sin^2 \theta}}{u_2 \sqrt{1 - u_1^2 \sin^2 \theta} + u_1 \sqrt{1 - u_2^2 \sin^2 \theta}}$$

reflection coefficient for waves reflected at  $S_{12}$ .

$$\delta_a = (4\pi a/\lambda_v) \frac{\sqrt{1 - u_1^2 \sin^2 \theta}}{u_1}$$

phase delay in top layer.

Expressing  $u_1$  in terms of the skin depth,  $d_1$ , in the top layer gives  $u_1 = kd_1/2$ . For a resistivity of 100-ohm-m, and for frequencies between 5 and 20 kc, the

skin depth varies from 70 to 35 m. Typical values for the thickness of the top layer are several meters. If the thickness is small compared to a skin depth, the ratio of the fields is very nearly

$$\frac{E_{\text{total}}}{E_{\text{direct}}} = 1 + \frac{\rho_{01} + \rho_{12}}{1 + \rho_{01}\rho_{12}} = \frac{2 \cos \theta}{\cos \theta + \sqrt{1/u_2^2 - \sin^2 \theta}} \quad (14)$$

which is the same as expression (12) derived for the case of the homogeneous earth. Thus, the influence of a good conducting layer can be neglected if its thickness is very much less than a skin depth.

The magnitude of the ratio of the total field directly above the antenna to the free-space field for a relative capacity of 6 is plotted in figure 6 as a function of the product of frequency and resistivity.

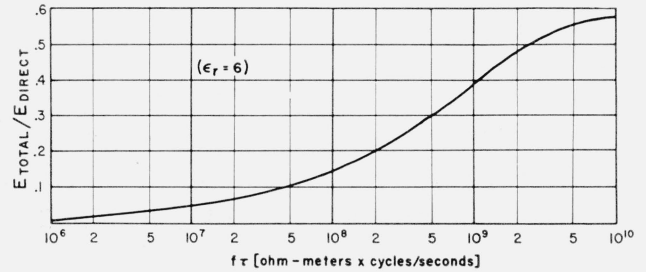


FIGURE 6. Magnitude of ratio of total field directly above the antenna to free-space field.

For the case of a stratified earth, the reflection method becomes cumbersome. This case is most readily solved by the wave method in which the field is resolved into traveling waves. By assuming solutions in each layer and matching the fields at the interfaces, one can obtain solutions for the fields directly above a horizontal antenna of arbitrary length. Wait has applied this method to a long wire filament and has obtained an expression for the electric field on the surface of the stratified medium [7].

## 2.1. Experimental Results

The properties of a horizontal half-wave antenna were investigated experimentally with three antennas located over ground with varying electrical properties.

The first antenna, half-wave resonant at 197 Mc, was located over dry rocky soil. Field strength measurements were made in the perpendicular bisector plane of the antenna. Figure 7 shows the theoretical and measured radiation patterns in this plane. By noting the ratio of maximum to minimum field strength directly over the antenna as the height of the antenna was varied, it was possible to calculate the relative capacity of the underlying ground. From (11):

$$\frac{E_{\text{max}}}{E_{\text{min}}} = \frac{1 - \rho}{1 + \rho} = \frac{1}{u} = \sqrt{\epsilon_r}, \quad (\rho < 0) \quad (15)$$

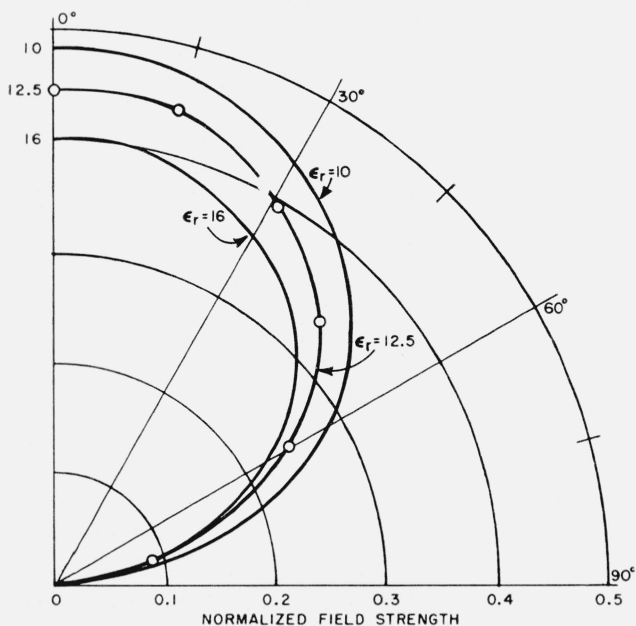


FIGURE 7. Field pattern of  $\lambda/2$  antenna over a plane earth  $h=0$  (calculated results for  $\epsilon_r=16, 10$  and measured values for  $\epsilon_r=12.5$ ).

Using a value of 12.5 for the relative capacitivity it is seen that the radiation pattern of the antenna is in good agreement with the theoretical result given by (4).

The input resistance of the antenna was also measured as a function of antenna height. From figure 8 it is seen that the resistance fluctuated about 70 ohms when the height was greater than  $\lambda/4$ , but increased rapidly when the height approached zero. At a height of 1.5 cm the input resistance was 80 ohms. The rise in resistance may be attributed to increased ground losses.

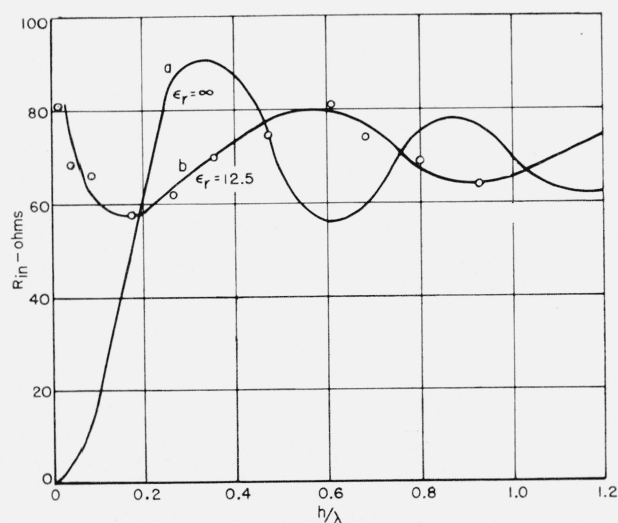


FIGURE 8. Input resistance of a half-wave antenna above a plane earth.

- (a) Calculated for  $\epsilon_r=\infty$   
 (b) Experimental for  $\epsilon_r=12.5$ .

A second antenna approximately 2,000 m in length was constructed above ground of relative capacitivity  $\epsilon_r=6$  or 7 and resistivity 137 ohm-m. The average height of the antenna was 1 m and it was resonant at 60 kc. The input resistance of the antenna (including 24 ohms copper loss) was 127 ohms. Changing the average height of the antenna to 3.4 m reduced the input resistance to 79 ohms. This change in resistance may be attributed almost entirely to the reduction in ground losses.

The third antenna was erected at approximately the same site as the second antenna and consisted of a wire 8,000 m long, supported about 3.4 m above the ground. By locating switches along the wire, it was possible to tune the antenna to different frequencies (simply by opening the appropriate pair of switches). The antenna was thus half-wave resonant in the frequency range between 18 kc and 250 kc. The vertically polarized field at the surface of the ground was in excellent agreement with the theoretical pattern of figure 4. The wave tilt was found to be very small as expected for this type of terrain. No vertically polarized field could be detected at the surface of the ground in the equatorial plane of the antenna.

The input resistance to the antenna at 18 kc was 82 ohms, 20 ohms of which was the estimated copper loss. The quality factor,  $Q$ , of the antenna was measured to be 12 at this frequency.

Several continuous-wave, vertical-incidence, ionospheric-sounding experiments using this antenna were conducted by Bergman et al. [8]. The antenna was driven by a 800-w transmitter which was tunable over a frequency range from 14 to 70 kc. The receiving site was located at a distance of 64 km from the transmitter in the perpendicular bisector plane of the transmitting antenna. Since no ground wave existed in this plane, it was possible to use two crossed dipoles to directly detect the relative amplitude and phase of the downcoming skywave, without subtracting a ground-wave component.

The dipoles were each 30 m in length and were oriented parallel and perpendicular to the vertical plane of the transmitting antenna. This orientation made it possible to record directly the skywave components polarized parallel to and normal to the plane of incidence.

By transmitting a continuous signal, data on the variations in height of the ionosphere were recorded. This was accomplished by comparing the phase of the received signal with a reference phase signal transmitted over a direct line-of-sight vhf communication channel.

The geometry of the sites is shown in figure 9. The particular spacing and orientation was governed by the geography of the area, and the requirement of a line of sight between stations. A block diagram of the complete system is shown in figure 10.

The experimental antennas thus made it possible to verify the theoretical radiation fields of a half-wave antenna from eqs (4) and (10). The rapid increase in antenna resistance as the antenna height approached zero is attributed to the increase in ground losses. This result was predicted by Sommerfeld and

Renner [9] who determined the radiation and earth absorption of a dipole antenna over a finite conducting earth. Their results are basically those presented in figure 8. This rapid increase is due to the extremely high fields in the immediate vicinity of the antenna wire. Thus, in order to prevent excessive losses, a horizontal vlf antenna should be placed at least several meters above the earth's surface.

### 3. Form of the Current Distribution

Coleman [10] has shown that the propagation constant of waves traveling along a wire located at the interface between two media is strongly affected by the intrinsic propagation constants of the two media. In the case of actual ground constants encountered at very low frequencies, the propagation constant for waves traveling along a wire located at an earth-air interface is

$$\Gamma \cong \frac{1}{2} (1+i) \sqrt{\sigma_2 \mu \omega} \quad (16)$$

However the change in propagation constant from the free-space value to the interface value is expected to be quite sharp, the transition taking place in a few diameters of the wire [5].

The horizontal, half-wave antenna discussed in this paper was mounted on poles, several meters above the earth. The fields of eqs (4), (6), and (10) were calculated assuming the antenna to lie on the earth (i.e.,  $h=0$ ). This approximation is justified when it is considered that at very low frequencies the wavelength is at least 10 km, so that  $\lambda \gg h$ .

On the other hand, the criterion that the antenna wire be more than a few wire diameters above the earth is also satisfied, i.e.,  $d \ll h$ . Since the prop-

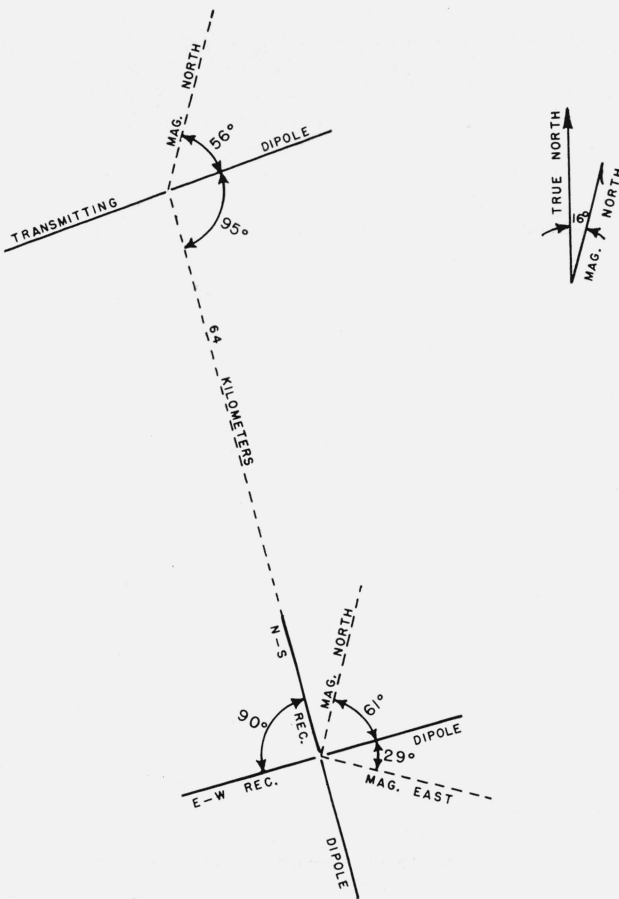


FIGURE 9. Geometry of the transmitting and receiving antennas.

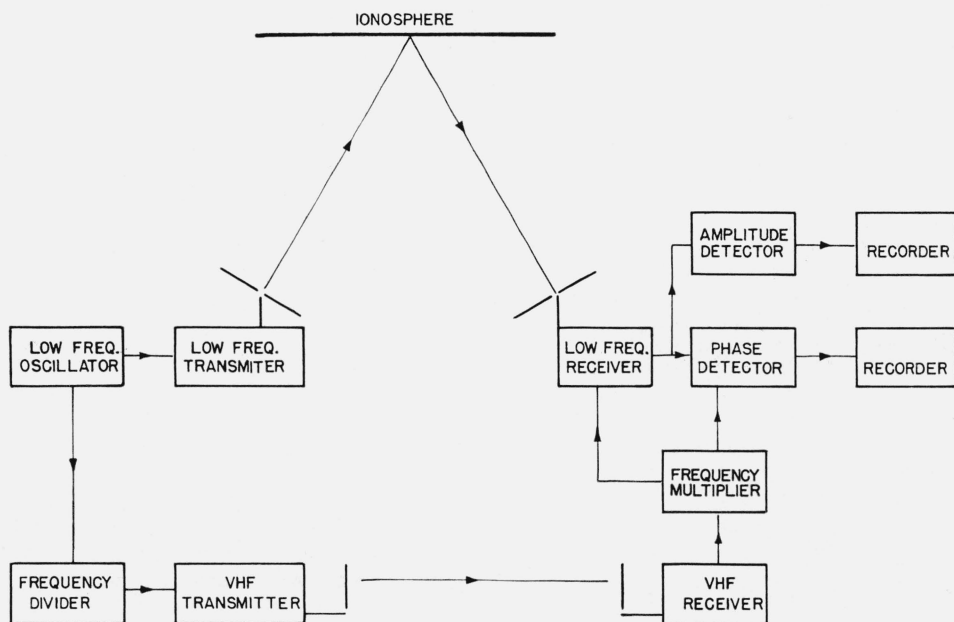


FIGURE 10. Block diagram of the transmitting and receiving system.

agation constant should then be close to that of free space, the approximation has been made that the current distribution on the horizontal, half-wave antenna is  $I_{rms}(x) = I_0 \cos kx, -\frac{\lambda}{4} \leq x \leq \frac{\lambda}{4}$ . To determine the validity of this approximation, an experiment was performed using the antenna resonant at 60 kc. The antenna was approximately 2,000 m long and had an average height of 1 m. The wire diameter was approximately  $\frac{1}{2}$  cm. The antenna was driven at its center with a power oscillator, and the antenna current distribution was determined by inserting a thermal ammeter at a number of points along the antenna wire. The accuracy of the current distribution which was obtained was limited by the linearity of the ammeter and any small fluctuations of the oscillator power level which may have occurred during the course of the measurements. Within the estimated accuracy of 5 percent for the experiment, no departure from a cosinusoidal current distribution could be detected.

A second experiment was performed with a 10 Mc antenna mounted 1 m above the ground with virtually the same results as for the 60 kc antenna.

Furthermore, for the high values of ground resistivity which are of interest, and with the antenna located several meters above the earth's surface, any departure from the cosinusoidal current distribution should be pronounced only towards the ends of the antenna where the magnitude of the current is small. The authors believe that the departure from the assumed cosinusoidal current distribution would have only a very minor if not negligible effect on the values of the radiation fields of eqs (4), (6), and (10).

#### 4. Ground Resistivity

For antennas of the type being considered, it has been shown that the product of the earth's resistivity and the excitation frequency must be high to obtain a reasonable value for the radiated fields (see fig. 6). In order to find a site with extremely high ground resistivity, measurements were made at a number of locations in Central and Southern California (see fig. 11). The resistivity measurements were made by the four-electrode method [11]. The four electrodes are placed in the ground at specified distances

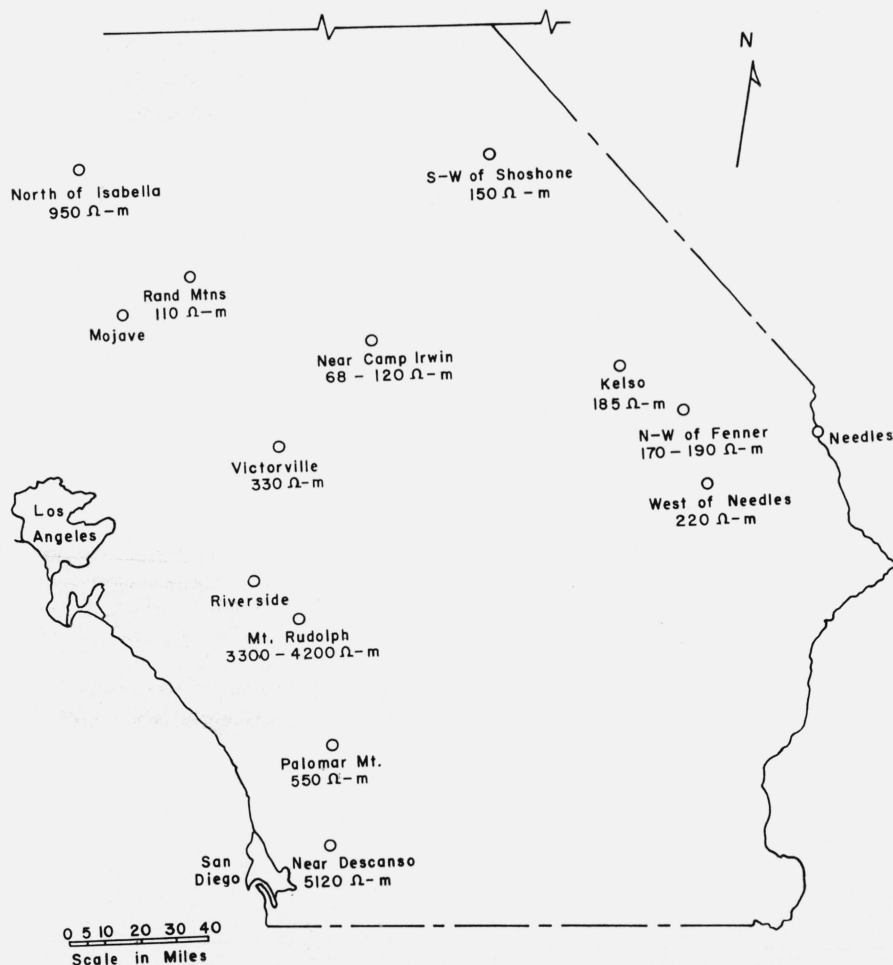


FIGURE 11. Southern California ground resistivity measurements.

apart, and a current is passed between the outer electrodes while the potential difference between the inner two is measured. From this measurement, the ground resistivity can be determined.

The resistivity measurements were made in three general areas of California—the Mojave Desert region, a triangular section (indicated by the numeral II in fig. 12) of the Peninsular Range province, and a section of the Sierra Nevada Mountains east of Fresno.

The Mojave Desert is a broad interior region of isolated mountain ranges separated by expanses of desert plains. It has an enclosed drainage system with playas, except for the bordering Colorado River province on the east. There are two important fault trends: the NW-SE trend is the more prominent, while the E-W trend is secondary. The province is wedged in a sharp angle between the Garlock fault and the San Andreas fault (see fig. 12).

The Peninsular Range province consists of a series of ranges separated by longitudinal valleys, trending

NW-SE. The trend of the topography is like that of the coast ranges, but the geology is more like that of the Sierra Nevada. The dominating rocks are granitic, intruded into older metamorphic series. The coastal area receives 11 to 18 in. of rainfall per year while some of the higher mountains receive as much as 50 in./yr.

The Mojave Desert resistivity measurements were made in areas which: (1) Received very little rainfall; (2) had a very-low water table (as low as 2,300 ft below the surface); and (3) were underlain by granitic rocks. However, the resistivity values were much lower than expected. These values ranged from 68 to 330 ohm-m (see fig. 11).

The low values of resistivity are attributed to the extensive faulting which occurs in the province (see fig. 12). The rocks are badly fractured, and these fractures contain water which is held by capillary forces. Thus the resistivity is low, even though the area receives little rainfall—as low as 0.5 to 2 in./yr in some sections.

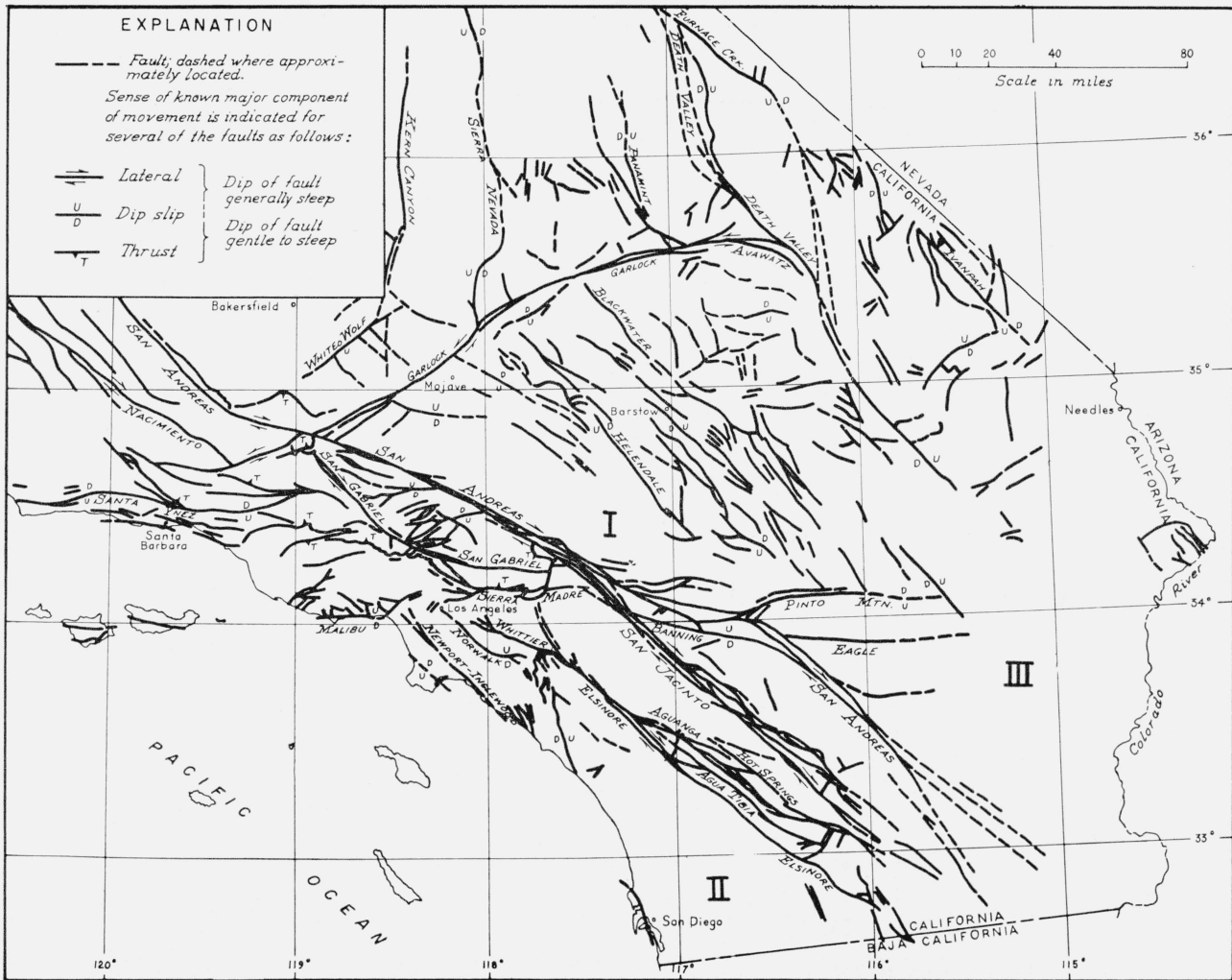


FIGURE 12. Map showing major faults in a large part of Southern California.

Based mainly on mapping and compilation by C. R. Allen, T. L. Bailey, T. W. Dibblee, Jr., D. F. Hewett, R. H. Jahns, and L. F. Noble.



The triangular section indicated by the numeral II in figure 12 is a large block or batholith which is free of faulting. Large areas of relatively unfractured granite were found in both this triangular section and the Sierra Nevada Mountains. The resistivity values for these areas were found to range from 2,100 to 5,120 ohm-m. It is concluded that for high values of resistivity, the rock formations must be relatively unfractured, while the amount of annual rainfall and other climatic conditions are of little significance.

It might be inferred from figure 12 that there is little faulting in the areas indicated by the numerals I and III. However, this is not the case. The faults are not shown in these areas, because deep alluvium deposits prevent their accurate location.

## 5. Power-Line Antenna

In 1955 a program of research was initiated by the California Institute of Technology under the sponsorship of the Office of Scientific Research of the Air Research and Development Command. The purpose of this research was to investigate various aspects of vlf propagation.

Initially it was proposed to construct a horizontal half-wave antenna. It was subsequently proposed, however, that a commercial power line might be used as the transmitting antenna. This proposal led to the analysis, design, and construction of a unique vlf antenna system. This system employed a single-phase, medium voltage, commercial power line. The antenna section was isolated from the rest of the distribution system by parallel resonant circuits, or line-traps (see fig. 13). Two of these traps were located at each end of the half-wavelength antenna section, and two at the center of the antenna. The end traps served principally to prevent the radio-frequency energy from coupling past the antenna section into the remainder of the power distribution system. The center traps isolated the antenna section into two halves so that it could be fed as a balanced, center-fed antenna. The radiofrequency traps were designed to present a negligible impedance to the flow of 60 cps power and a maximum impedance to the radiofrequency power. In this manner it was possible to draw 50 kw of 60 cps power from the center of the antenna section to drive the transmitter while simultaneously radiating vlf energy from the same section of line.

The radiation patterns of the power-line antenna

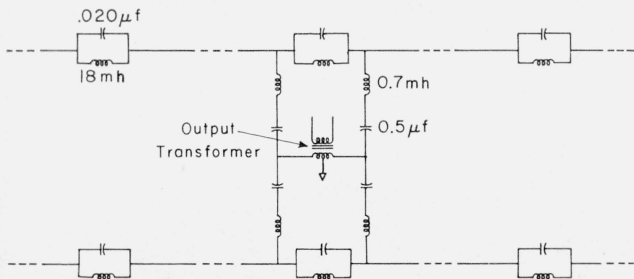


FIGURE 13. Schematic diagram of the power-line antenna system.

are virtually identical to those of figures 2, 3, and 4 [12].

The power-line antenna was used primarily for ionospheric sounding experiments at 8.4 kc. Measurements of the amplitude variations of the reflected sky wave signal revealed information about the lower regions of the ionosphere. Transcontinental detection of the 8.4-kc signal from California to Cambridge, Mass., indicated that the antenna system is also capable of long-range propagation.

## 6. Conclusions

The radiation field of a half-wave, linear antenna located above a plane earth of finite conductivity consists of: (1) A horizontally polarized field in the midplane perpendicular to the antenna, which is zero in the plane of the earth; and (2) a vertically polarized groundwave which is maximum in the direction of the axis of the antenna and zero at right angles to the antenna. This radiation field, given in eq (4), (6), and (10) has been confirmed by experimental data. The nature of its radiation field makes this simply constructed antenna extremely useful in ionospheric propagation experiments. The radiation is maximum in the vertical direction, and in the midplane of the antenna there is no direct ground-wave radiation to interfere with the reflected sky-wave information.

To obtain maximum radiation fields, it is necessary to locate the antenna over ground of high resistivity. This type of ground is primarily located in geological areas free of faulting.

## 7. References

- [1] A. Sommerfeld, The propagation of waves in wireless telegraphy, *Ann. Physik.* **28**, 665 (March 1909).
- [2] H. Weyl, The propagation of electromagnetic waves over a plane conductor, *Ann. Physik.* **60**, 481 (Nov. 1919).
- [3] J. A. Stratton, *Electromagnetic theory*, 573 (McGraw-Hill Book Co. Inc., New York, N.Y., 1941).
- [4] K. A. Norton, The physical reality of space and surface waves in the radiation field of radio antennas, *Proc. IRE* **25**, 1192 (Sept. 1937).
- [5] J. R. Wait, Radiation from a ground antenna, *Can. J. Technol.* **32**, 1 (Jan. 1954); also, Low-frequency radiation from a horizontal over a spherical earth, *Can. J. Phys.* **34**, 586 (1956).
- [6] J. R. Wait, Excitation of surface waves on conducting stratified dielectric-clad and corrugated surfaces, *J. Research NBS* **59**, 365 (Dec. 1957) RP2807.
- [7] J. R. Wait, The fields of a line source of current over a stratified conductor, *Appl. Sci. Research [B]* **3**, The Hague, Martinus Nijhoff (1953).
- [8] C. W. Bergman, R. S. Macmillan, W. H. Pickering, A new technique for investigating the ionosphere at low and very low frequencies, (*Rocket Exploration of the Upper Atmosphere*, Interscience Publishers, Inc., New York, N.Y., 1954).
- [9] A. Sommerfeld, F. Renner, Strahlungsenergie und erde absorption bei dipole antennen, *Ann. Physik.* **41**, 1 (Jan. 1942).
- [10] B. L. Coleman, Propagation of electromagnetic disturbances along a thin wire in a horizontally stratified medium, *Phil. Mag.* **41**, 276 (1950).
- [11] W. R. Smythe, *Static and dynamic electricity*, 241 (McGraw-Hill Book Co., Inc., New York, N.Y., 1950).
- [12] W. V. T. Rusch, A new transmitting antenna system for very low radio frequencies, Ph.D. Thesis, Calif. Inst. Technol. (1959).

BOULDER, COLO.

(Paper 64D1-34)